Research Article

Theresa S. Bonenberger*, Jörg Baumgart and Cornelius Neumann

Angular and spatial color mixing using mixing rods with the geometry of a chaotic-dispersive billiard system

DOI 10.1515/aot-2015-0056
Received November 27, 2015; accepted January 18, 2016; previously published online February 12, 2016

Abstract: For mixing light from different colored LEDs, an optical color mixing system is required to avoid colored shadows and color fringes. Concerning the different color mixing systems, mixing rods are widespread as they provide very good spatial color mixing with high efficiency. The essential disadvantage of mixing rods, so far, is the lack of angular color mixing. The solution presented in this publication is the application of a chaotic-dispersive billiard's geometry on the cross section of the mixing rod. To show both the spatial and the angular mixing properties of a square and a chaotic-dispersive mixing rod, simulations generated by the raytracing software ASAP are provided. All results are validated with prototype measurements.

Keywords: chaotic billiards; LED color mixing; mixing rods.

OCIS Codes: 330.1690; 350.4600.

1 Introduction

Many applications, e.g. projection lighting, mood lighting, theater lighting, and therapeutic lighting are demanding color tuneable light sources. Principally, these sources can be used for adjusting every color within the gamut of the LEDs. Additionally, it can perform white light with the possibility to adjust different color temperatures. To realize a tuneable light source with LEDs, an optical mixing system is required. Because all LEDs are spatially separated, this spatial separation will be converted into an angular separation by conventional collimating optics. This means to accept the occurrence of colored shadows and color fringes. Accordingly, illuminating an object with several distinct LEDs without any optics will also produce colored shadows. There are different methods to mix the light of several LEDs, e.g. using dichroic filters [1–3], diffraction gratings [4], diffusers [5], and micro lens arrays [6–8]. Very often, mixing rods are used because they provide very good spatial color mixing with a high efficiency [9–12]. One essential disadvantage of mixing rods is the inability of good angular color mixing. Thus, it is desirable to implement a mixing rod combining both a very good spatial and angular color mixing. This can be done by applying the geometry of a chaotic dispersive billiard system [13] to the cross section of the mixing rod.

2 Materials and methods

Mixing rods are a special type of light guides, which homogenize light by guiding it with multiple reflections. Usually, mixing rods are solid, and the material is PMMA (Polymethylmethacrylat). For mixing the LEDs' light by means of mixing rods, the only need are the LEDs and the mixing rod and no further additional optics. The coupling of the LED light into the mixing rod can be done by placing a LED with a flat protection glass in front of the rod's entrance face. In this publication, the LED Ostar Stage from the company Osram [14] is used for simulations and experimental setups.

The LED Ostar Stage is a four-chip LEDs with the colors red, green, blue, and white. Figure 1A shows a photo of the LED, and Figure 1B shows the arrangement of the different chips as a spot diagram. Each chip has approximately a size of 1 mm^2 with a distance of approximately 1 mm between them. All simulations were done with the rayfiles provided by Osram [15].

***Corresponding author: Theresa S. Bonenberger,** Hochschule Ravensburg Weingarten, ZAFH LED OASYS, Doggenriedstraße, 88250 Weingarten, Germany; and Karlsruhe Institute of Technology, Department of Electrical Engineering and Information Technology, Light Technology Institute, Engesserstr. 13, 76131 Karlsruhe, Germany, e-mail: Theresa.Bonenberger@hs-weingarten.de
Jörg Baumgart: Hochschule Ravensburg Weingarten, Doggenriedstraße, 88250 Weingarten, Germany
Cornelius Neumann: Karlsruhe Institute of Technology, Department of Electrical Engineering and Information Technology, Light Technology Institute, Engesserstr. 13, 76131 Karlsruhe, Germany

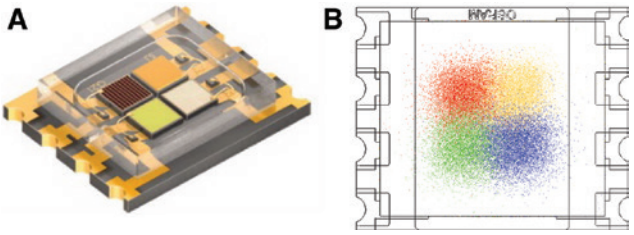

Figure 1: (A) Photo of the LED Osram Ostar Stage [14]. (B) Spot diagram of the LED with the LED profile to show the arrangement of the different colored chips.

The spatial and angular mixing properties are determined by the length of the mixing rod and the shape of the cross section. The efficiency of a mixing rod is determined by the spectral transmission of the mixing rod and the coupling efficiency. Primarily, the spectral transmission is limited by the Fresnel reflections at the entrance and exit face because the absorption losses of PMMA are theoretically negligible. Owing to small scratches and roughness on the surface, losses can occur because the critical angle of total internal reflection will not be fulfilled any more. The coupling efficiency depends on the acceptance angle of the mixing rod. By using PMMA, theoretically, the complete light emission of a LED, positioned close to the entrance surface, can be coupled into and guided through the mixing rod. The LED Osram Ostar can be positioned very close to the entrance surface, but still there remains a little distance because of the glass window between the LED-emitter surface and entrance surfaces of the mixing rod.

To show the basic concepts and to analyze the color-mixing properties of square and dispersive mixing rods, the raytracing software ASAP [16] was used to get the illuminance and the luminous intensity distributions. Owing to numerical noise, high frequent spatial and angular variations could not have been detected. All the illuminance and the luminous intensity distributions in the publication are made with the ASAP averaging feature, smoothing the distribution data by averaging over 1 adjacent pixel.

To evaluate the color-mixing properties of a mixing rod, it is only necessary to assess the angular and spatial mixing quality, without considering the wavelength because light propagation in a mixing rod is independent of the wavelength. To quantify the spatial and angular uniformity, a merit function based on the 'flux compensation approach' is used [17, 18]. The 'flux compensation approach' is made to compare one-dimensional light distributions. To obtain a merit function for color uniformity, the 'flux compensation approach' was extended to compare two-dimensional light distribution of two spatially separated LED chips at the mixing rod's exit face. The description and mathematical background of the merit functions can be found in another publication [19]. Light distributions, corresponding to each other, indicate good color mixing, and the merit function converges to zero. An increasing merit function indicates an increasing difference between two light distributions. To evaluate spatial color mixing, the illuminance distributions are used with the merit function M_E, whereas the luminous intensity distributions are used to evaluate angular color mixing with the merit function M_I. In this paper, the light distributions of the LEDs at the position of the red and the green LED from the LED Osram Ostar Stage were used.

To illustrate the reasons why dispersive mixing rods show good angular mixing properties, while square mixing rods show bad angular mixing properties, the shape of the cross section is considered to represent a two-dimensional mathematical billiard system. Such a system characterizes a plane area (the billiard table) with a material point, moving with constant speed in this area, until it collides with the boundary. At the boundary, an elastical reflection takes place, according to the law of reflection. After the reflection, the material point moves straight forward until it repeats colliding with the boundary [20].

3 Square mixing rod

Square mixing rods are solid light guides with a square cross section. They provide good spatial color mixing. In this section, the light distributions of two spatially separated LED chips from the LED Osram Ostar Stage (see Section 2) are shown after the propagation through a mixing rod with a 4 mm×4 mm square cross section and a total length of 50 mm.

3.1 Spatial mixing properties

The basic concept of spatial color mixing with a mixing rod is often explained with an approach called 'mirror tiling' [21, 22]. This approach considers the illuminance distribution, which would occur if the mixing rod is taken away. This 'without mixing rod' illuminance distribution is overlapped by multiple reflection, and at the exit face, a uniform distribution appears. However, not all cross sections provide spatial uniformity. Only the 'mirror-tiled' shapes, including squares, rectangles, hexagons, and equilateral triangles, fulfill this requirement.

A round-, a hexagonal-, and a square-shaped mixing rod were analyzed. The round mixing rod showed no uniform illuminance distribution because the cross section has no mirror-tiled shape. The square and the hexagonal mixing rod both have mirror-tiled shapes, and therefore, spatial color mixing is possible with both of the rods. However, the length of the hexagonal mixing rod has to be longer than the length of the square mixing rod to obtain full spatial uniformity. Consequently, every mixing rod with a mirror tiled cross section requires a certain length to achieve complete spatial uniformity. This length is determined by the number of the symmetry axes of the cross section, affecting the reflections. For instance, considering the geometry, the square shows four symmetry axes; the two diagonal axes and the vertical and horizontal axes through the center of the cross section. However, the two diagonal symmetry axes do not affect the reflections because rays colliding with the edges are not defined. Thus, there are only two symmetry axes

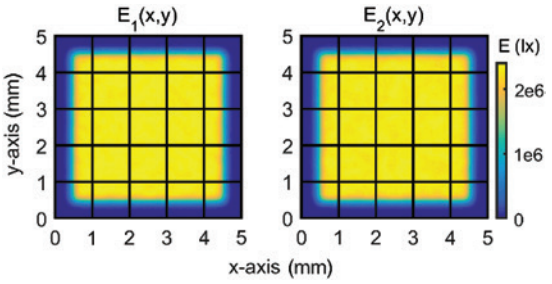

Figure 2: Simulated illuminance distribution at detector surface of two light sources, placed at different positions on the entrance face, after the propagation through a square mixing rod.

affecting the reflections. As the square mixing rod shows less symmetry axes than the hexagonal one, it presents better spatial mixing properties.

In Figure 2, the illuminance distributions of two spatially separated LED chips from the LED Osram Ostar Stage (see Section 2) on a detector at the exit face of a 4 mm×4 mm square mixing rod with 50-mm length are shown. As they are identical, the square mixing rod demonstrates good spatial color mixing, and the merit function is $M_E<10^{-3}$.

3.2 Angular mixing properties

Homogeneous angular color mixing does not occur with square mixing rods. The multiple reflections generate multiple images of the LED, causing the so-called 'kaleidoscope image,' which describes a pattern of the light source extension and their position, in dependency on the cross section. With increasing length, the structure of the kaleidoscope pattern becomes more fine grained, but still remains.

Figure 3 shows the luminous intensity distribution of two spatially separated LED chips from the LED Osram Ostar Stage (see Section 2) at the exit face of a 4 mm×4 mm square mixing rod. The distribution shows solid angles with low luminous intensity and solid angles with high luminous intensity, caused by the kaleidoscope effect. Both kaleidoscope patterns are similar, but angularly shifted. As there is a big difference between the luminous intensity distribution, the merit function is M_I=12.2.

The kaleidoscope pattern is caused by the regular motions of the light trajectories. This is illustrated in a square billiard with two ray trajectories, starting with a very small azimuth angle difference of $\varepsilon=10^{-6}$°, shown in Figure 4. Because the motions of the trajectories are regular, similar starting conditions of the rays lead to similar motions of the trajectories.

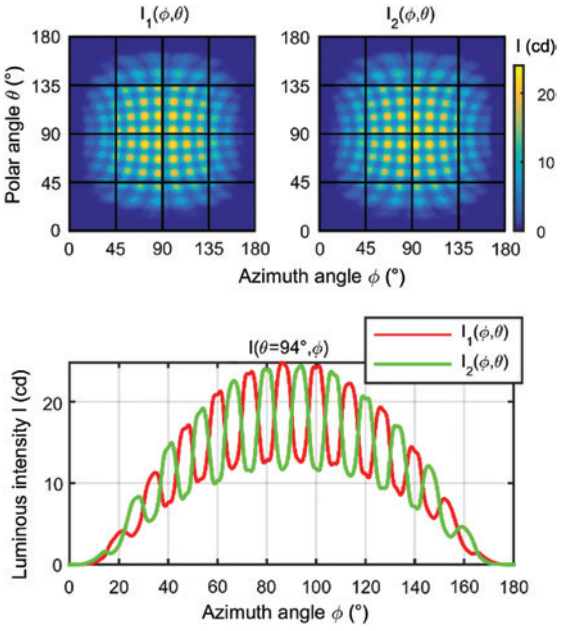

Figure 3: Simulated luminous intensity distribution of two light sources, placed at different positions on the entrance face, after the propagation through a square mixing.

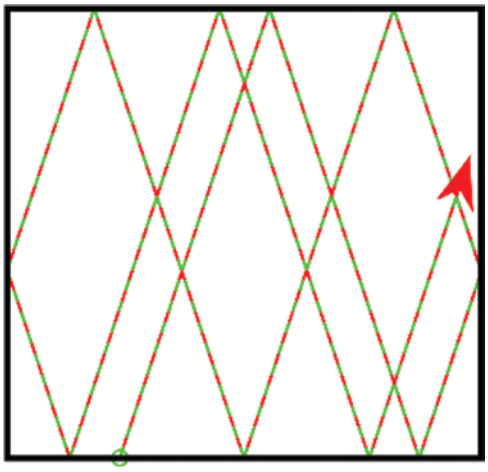

Figure 4: Illustration of two trajectories, which have starting points with an infinitesimal small angle difference, moving in a square billiard.

4 Chaotic-dispersive mixing rod

Dispersive mixing rods are solid light guides with a cross section corresponding to the geometry of a dispersive billiard [13]. The dispersive billiard belongs to the class of chaotic billiards. All boundaries of such a billiard are convex (the geometrical center of each boundary is outside the billiard area). Such billiards are called dispersive because a parallel ray bundle is dispersed after

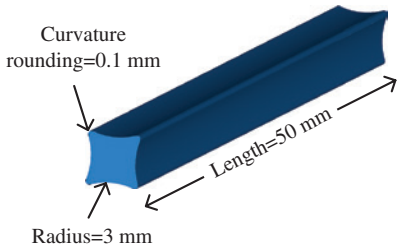

Figure 5: Perspective figure of the dispersive mixing rod.

a reflection at the boundary. In this section, a chaotic-dispersive mixing rod with the dimensions shown in the perspective view in Figure 5 is analyzed.

4.1 Spatial mixing properties

Contrary to the square mixing rod, the chaotic-dispersive mixing rod, see Figure 5, has no mirror-tiled shape. Nevertheless, it provides a uniform illuminance distribution at the exit face of the mixer. This is illustrated in Figure 6, which shows the illuminance distributions of two spatially separated LEDs on a detector at the exit face of the dispersive mixing rod. As the illuminance distributions are identical, it can be concluded that the LED's light is spatially mixed, which is confirmed by the merit function of $M_E<10^{-3}$.

This is generated by the symmetry axes of the geometry. The mixing rods with mirror-tiled shapes show better spatial color-mixing properties with a decreasing number of symmetry axes. However, the cross section of the dispersive mixing rod has no symmetry axes, affecting the reflections. Considering the geometry, the cross section of the dispersive mixing rod has four symmetry axes, like the square mixing rod. The two diagonal symmetry axes do not affect the reflections because a ray colliding with an edge is not defined. In contrast to the square mixing rod, the horizontal and vertical symmetry, referring to the geometrical center point of the geometry, only shows an

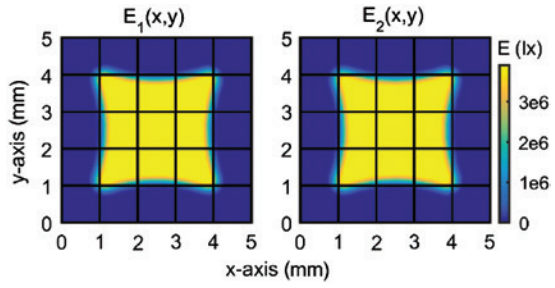

Figure 6: Simulated illuminance distribution at detector surface of two light sources, placed at different positions on the entrance face, after the propagation through the dispersive mixing rod.

effect on rays, moving exactly on the axes. Thus, they are negligible. In summary, this complete symmetry breaking leads to very good spatial mixing properties.

4.2 Angular mixing properties

By using the chaotic-dispersive mixing rod with a cross-sectional shape of a chaotic billiard, angular color mixing can be made. The basic concept of angular color mixing with a dispersive mixing rod is illustrated in Figure 7. Two trajectories are shown, starting with an infinitesimal small angle difference. In contrast to the square mixing rod, the angle difference between the two trajectories increases exponentially with every reflection. Notably, this strong sensitive dependence on initial conditions is the fundamental property of every chaotic system.

With equation 1, the angle difference Δ between two trajectories after N reflections is calculated. The sensitivity of a dynamical system can be quantified with the so-called Lyapunov exponent σ. If the Lyapunov exponent is greater than zero, an infinitesimal small error ε grows exponentially and, therefore, indicates chaotic behavior.

$$\Delta(N)=\varepsilon e^{\sigma N} \tag{1}$$

The Lyapunov exponent is calculated with equation 2 with the so-called renormalization method [23, 24]. This is corresponding to an averaging over k developments of the angle difference between two trajectories. Therefore, a reference trajectory is calculated continuously. Furthermore, a neighbor trajectory is calculated for N reflections, starting with an infinitesimal small distance ε to the reference trajectory. Subsequently, it is replaced to the distance

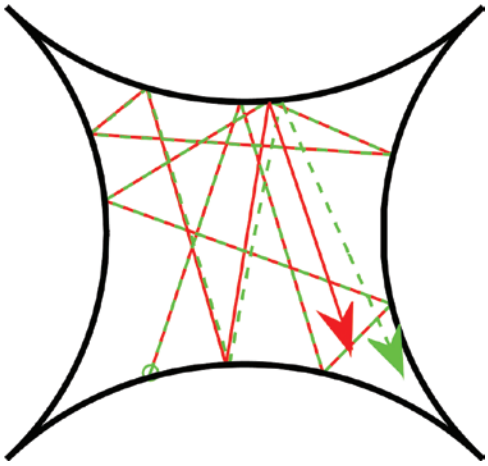

Figure 7: Illustration of two trajectories, which have starting points with an infinitesimal small angle difference, moving in a dispersive billiard.

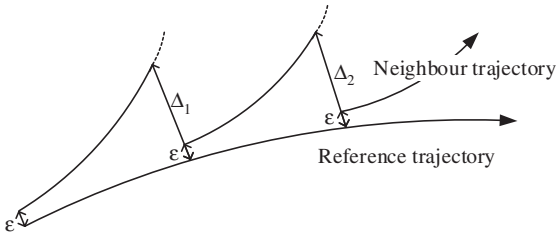

Figure 8: Schematic representation of the renormalization method for the calculation of the Lyapunov exponent.

ε after N reflections and restarted from there, like shown schematically in Figure 8.

$$\sigma = \frac{1}{kN} \sum_{i=1}^{k} \ln \frac{|\Delta_i|}{\varepsilon} \tag{2}$$

Note that the application of a dispersive billiard's geometry on the cross section of a mixing rod provides angular color mixing because all trajectories show chaotic motions. The higher the sensitivity of the cross section, the better is the result for angular color mixing. The sensitivity of a dispersive billiard is influenced by the radius of the convex boundaries. To achieve maximum sensitivity, the Lyapunov exponent is calculated for different radii, shown in Figure 9, for a billiard's edge length of 4 mm with N=3000 reflections.

Generally, the principle is that the smaller the radius is, the faster the trajectories move away from each other because the convex boundaries become more dispersive. However, by choosing the smallest possible radius, so that the convex boundary does not cut each other, the cusps are very narrow. Consequently, the distances between the reflections in the cusps are getting shorter, and with that, the trajectories move away from each other slower. The maximum Lyapunov exponent is σ=0.97 for a radius of r=3.9 mm. Of course, for real optics, such narrow cusps are anyway not manufacturable and are, therefore, rounded.

In Figure 10, the luminous intensity distributions of two spatially separated LEDs at the exit face of the dispersive mixing rod (dimensions can be found in Figure 5) are shown. Both distributions are similar, which indicates good angular color mixing. Only the direct light has no reflection and cannot be mixed in this way. Therefore, the merit function is M_I=4.2 and not 0. Accordingly, one improvement is to increase the mixing rod's length, even though complete mixing cannot be achieved this way. The principle solution of this problem is the bending of the mixing rod [25, 26].

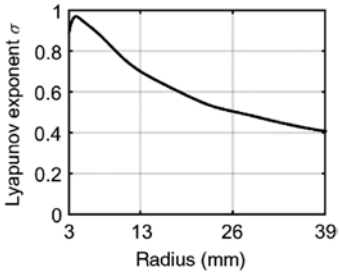

Figure 9: Dependency of the Lyapunov exponent on the radii of the convex boundary for a dispersive billiard.

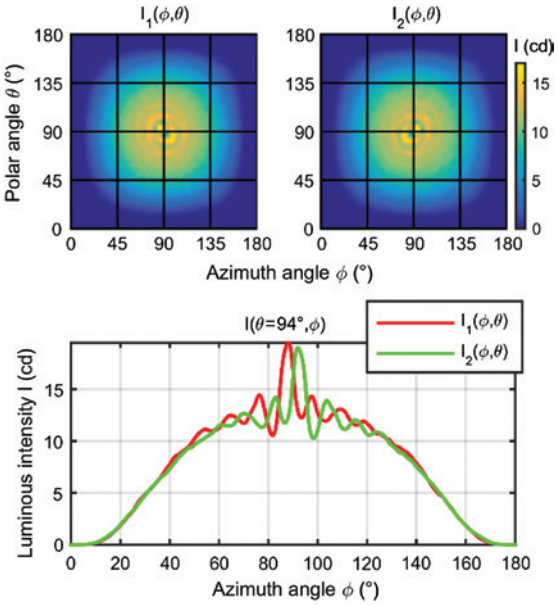

Figure 10: Simulated luminous intensity distribution of two light sources, placed at different positions on the entrance face, after the propagation through a dispersive mixing rod.

The luminous intensity distribution of a bended mixing rod is shown in Figure 11. For the simulation, a dispersive mixing rod with the same cross section as shown in Figure 5 was used, consisting of two straight parts of each 50 mm and a bended part in the middle with a radius of 70 mm and an arc of 25°. It is important that in front and behind the bended part, each straight section is long enough to mix all light rays. Both luminous intensity distributions are identical, which indicates the corresponding light sources are angularly mixed completely. This is confirmed by the merit function which is M_I<10^{-3}.

5 Measurement results and discussion

To validate the simulation results, prototypes of a square and a dispersive mixing rod were manufactured, and photometric measurements were done. The prototypes have

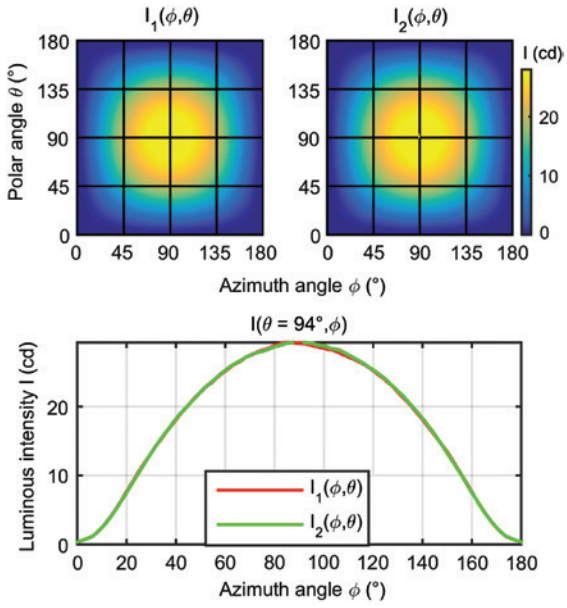

Figure 11: Luminous intensity distribution of two light sources, placed at different positions on the entrance face, after the propagation through a bended dispersive mixing rod.

the same dimensions as the simulated rods. To measure the luminous intensity distribution, a near-field goniophotometer was used. From the results of these measurements, rayfiles were generated for further analysis in the raytracing software ASAP. Thus, a direct comparison of simulated and measured light distribution was possible. As a light source for the measurements, the same LED as in the simulations, Osram Ostar Stage, was taken.

5.1 Spatial color mixing

Figure 12 shows the measured illuminance distributions on a detector surface at the exit face of the square mixing rod from two spatially separated LEDs. The distributions show a very small difference, which is confirmed by the merit function with M_E=0.07. This small spatial non-uniformity is caused because spatial mixing is done with the 'mirror-tiling' approach (see Section 3.1). As the prototype is hand manufactured, the cross section is not the perfect mirror-tiled geometry, though small non-uniformities occur. However, the distributions are almost similar, which confirms the simulation results that a square mixing rod shows good spatial mixing properties.

Figure 13 shows the measured illuminance distributions on a detector surface at the exit face of the dispersive mixing rod from two spatially separated LEDs. The distributions are similar, and therefore, the merit function is M_E=5*10^{-3}. Again, the simulation result, that a dispersive mixing rod shows good spatial mixing properties, is confirmed.

5.2 Angular color mixing

Figure 14 shows the measured luminous intensity distributions of two spatially separated light sources after the propagation through a square mixing rod. Both distributions show a similar kaleidoscope image, angularly shifted. Accordingly, the LEDs are angularly not mixed, and the merit function is M_I=16.6.

When comparing the simulation luminous intensity distribution from Figure 3 with the result of the measurements, a difference in the kaleidoscope images can be observed. The measured patterns are not as distinct as the simulated ones, especially for solid angles far away from the optical axes. This effect is caused by small scratches, dust particles, and roughness, of the mixing rod's hand polished surface. A ray reflecting at a small scratch or roughness will be scattered and distracted. Rays, which are only distracted, but still remain reflected into the mixing rod, cause a better angular mixing. However, rays scattered outside the mixing rod get lost.

Figure 15 shows the measured luminous intensity distributions of two spatially separated light sources

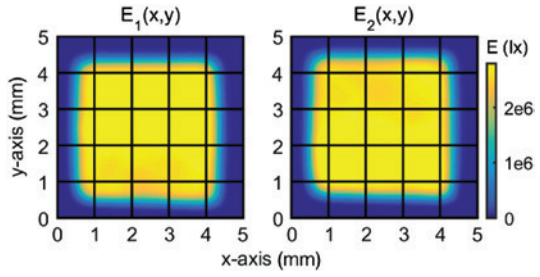

Figure 12: Measured illuminance distribution at detector surface of two light sources, placed at different positions on the entrance face, after the propagation through a square mixing rod.

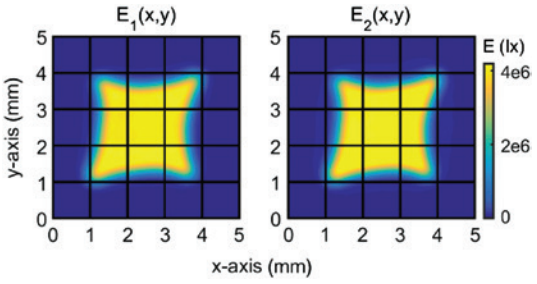

Figure 13: Measured illuminance distribution at detector surface of two light sources, placed at different positions on the entrance face, after the propagation through a dispersive mixing rod.

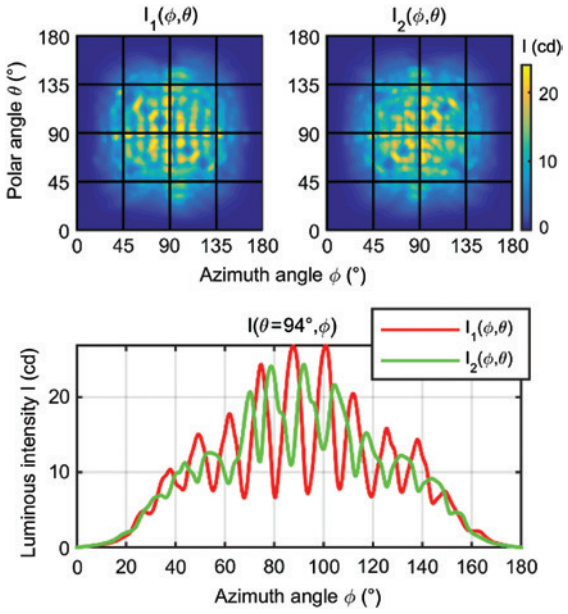

Figure 14: Measured luminous intensity distribution of two light sources, placed at different positions on the entrance face, after the propagation through a square mixing rod.

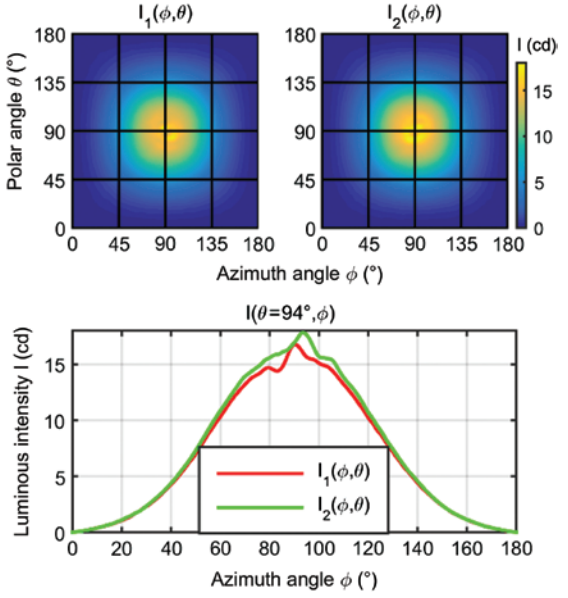

Figure 15: Measured luminous intensity distribution of two light sources, placed at different positions on the entrance face, after the propagation through a dispersive mixing rod.

after the propagation through a dispersive mixing rod. Both distributions are similar to each other, indicating that the sources are angularly mixed. Only the direct part of light shows no mixing because of the light guide's straight and unbent shape. Therefore, the merit function is M_I=2.8, which shows a better angular uniformity than the simulations.

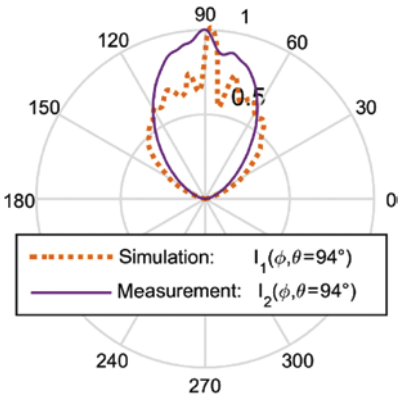

Figure 16: Simulated and measured normalized luminous intensity distribution of the red LED in the polar diagram after the transfer through a dispersive color mixing rod.

To compare the simulated luminous intensity distributions from Figure 10 with the measured ones, the measured and simulated results of the red LED are shown in Figure 16. First of all, the solid angle of the measured distribution is the smaller one. Analogical to the square mixing rod, the dispersive mixing rod is influenced by the same effect – by small scratches, dust particles, and roughness of the mixing rod's hand polished surface. Second, the rays close to the optical axes are angularly mixed much more in the real prototype than in the simulated one. As these rays are reflected only a few times, it can be concluded that in real systems, less reflections are needed to fulfill angular color mixing. Again, this is caused by roughness of the hand polished surface, making the system this way even more sensitive and, therefore, providing better angular color-mixing properties.

To obtain an impression of the visual color distribution, the photos in Figure 17 show the illumination of a detector surface, placed 0.5 m behind a (a) square mixing rod and (b) dispersive mixing rod. Beside the colored part of the direct light, the detector surface, illuminated with the dispersive mixing rod, shows a uniform white light distribution. In contrast, the detector surface, illuminated

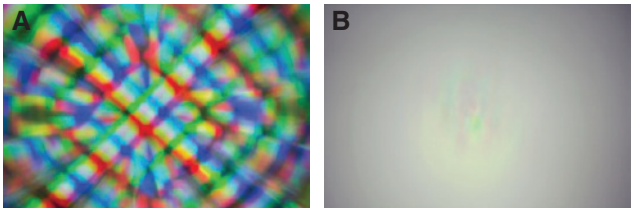

Figure 17: Photos show the illumination of a detector surface, placed 0.5 m behind the (A) square mixing rod and (B) dispersive mixing rod.

Table 1: Simulated and measured efficiencies of the square and dispersive mixing rod.

	Simulation η	Measurement η
Dispersive	0.81	0.51
Square	0.86	0.76

with the square mixing rod, shows as expected a colorful kaleidoscope image.

Table 1 lists the simulated and measured efficiencies of the square and the dispersive mixing rod. In simulation and measurement, the latter shows a lower efficiency than the square mixing rod. Owing to small scratches, dust particles, and roughness of the mixing rod's hand polished surface, the measured efficiencies are lower than the simulated ones. Another reason, which especially concerns the dispersive mixing rod, is that the entrance surface is very small compared with the LED size, and therefore, not all light is coupled into the mixing rod.

6 Conclusion

We presented a full angular and spatial color mixing by light guide rods for the first time. This was possible by applying the concept of chaotic dispersive billiards on the cross-sectional geometry of the light guide.

Conventional mixing rods, like square mixing rods, only provide spatial color mixing but no angular color mixing, due to the regular motion of the light trajectories. In contrast, light trajectories in dispersive mixing rods show chaotic motion, and therefore, color mixing is provided.

In addition, the small amount of direct light can be mixed by bending the rod.

All simulation results were validated with measurements of prototypes. Ultimately, considering the angular color uniformity, the measurements delivered even better results than the simulations.

Acknowledgments: This work has been conducted within the Research Association 'Zentrum für angewandte Forschung an Hochschulen' (ZAFH LED OASYS). The authors gratefully acknowledge the research grants of the state Baden-Württemberg and the European Union, European Regional Development Fund.

References

[1] E. Chen, Y. Feihong and T. Guo, Appl. Opt. 53, 1151–1158 (2014).
[2] S. Roelandt, L. Bogaert, Y. Meuret, A. Avci, H. De Smet, et al. in 'Proc. of SPIE 7723', (Brüssel, Belgien, 2010).
[3] R. van Gorkom, G. van Asb, G. Verbeek, G. Hoelen, R. Alferink, et al., in 'Proc. SPIE 6670', (San Diego, CA, 2007).
[4] C. L. Coleman and R. H. Weissman, Multi-chip LED color mixing by diffraction, USA Patent US 6,604,839 B2, 12 August 2003.
[5] T. R. Sales, S. Chakmakjian, D. J. Schertler and M. G. Morris, in 'Proc. of SPIE Vol. 5530', (Denver, USA, 2004).
[6] J. Chaves, A. Cvetkovic, R. Mohedano, O. Dross, M. Hernadez, et al., in 'Proc. of SPIE Vol. 8550', (Barcelona, 2012).
[7] J. Muschaweck, in 'Proc. of SPIE Vol. 7954', (San Francisco, USA, 2001).
[8] E. Chen, R. Wu and T. Guo, Opt. Commun. 321, 78–85, (2014).
[9] W. J. Cassarly and T. L. Davenport, in 'Proc. SPIE Vol. 6342', (Vancouver, Kanada, 2006).
[10] W. J. Cassarly, in 'Proc. SPIE 7103', (Glasgow, Schottland, 2008).
[11] C. Deller, G. Smith and J. Franklin, Opt. Exp. 12(15), 2004, (2004).
[12] F. Fournier, W. J. Cassarly and J. P. Rolland, Opt. Lett. 33, 1165–1167 (2008).
[13] Y. G. Sinai, in 'Proc. of the International Congress of Mathematicians', (Kyoto, Japan, 1990).
[14] Osram Opto Semiconductors, 'Osram Opto Semiconductors,' [Online]. Available: http://www.osram-os.com/osram_os/en/products/product-catalog/led-light-emitting-diodes/osram-ostar/osram-ostar-stage/le-rtduw-s2w/index.jsp. [Zugriff am 31 August 2015].
[15] Osram Opto Semiconductors, 'LED Information Base,' [Online]. Available: https://apps.osram-os.com/Characteristic. [Zugriff am 15 July 2015].
[16] Breault Research Organization, 'Breault Research,' Breault Research Organization, 2015. [Online]. Available: http://www.breault.com/software/about-asap. [Zugriff am 04 September 2015].
[17] S. Wendel, Spektrum der Lichttechnik, Bd. 7, (KIT Scientific Publishing, Karlsruhe, 2014).
[18] W. J. Cassarly, in 'Proc. SPIE 7652', (Wyoming, USA, 2010).
[19] T. S. Bonenberger, Spektrum der Lichttechnik, Bd. 11, (KIT Scientific Publishing, Karlsruhe, 2016). Available: dx.doi.org/10.5445/IR/1000051858.
[20] S. Tabachnikov, Geometrie und Billard, (Springer-Verlag, Berlin, 2013).
[21] M. Bass, Handbook of Optics, Bd. II, (McGraw-Hill Companies, Florida, United States, 2010).
[22] J. R. Koshel, Illumination Engineering, (John Wiley & Sons, New Jersey, 2013).
[23] J. Argyris, G. Fraus, M. Haase and R. Friedrich, Die Erforschung des Chaos, (Springer-Verlag, John Wiley & Sons, 2010).
[24] R. Worg, Deterministisches Chaos, (BI Wissenschaftsverlag, Mannheim, 1993).
[25] A. Gupta, J. Lee and R. J. Koshel, Appl. Opt. 3640–3648, (2001).
[26] T. Davenport, R. Hansler, T. Stenger, W. Cassarly, G. Allen, et al., in 'SAE International Congress and Exposition', (1998).

Theresa S. Bonenberger
Hochschule Ravensburg Weingarten, ZAFH LED OASYS, Doggenriedstraße, 88250 Weingarten, Germany; and Karlsruhe Institute of Technology, Department of Electrical Engineering and Information Technology, Light Technology Institute Engesserstr. 13, 76131 Karlsruhe, Germany
Theresa.Bonenberger@hs-weingarten.de

Theresa S. Bonenberger received her M.Sc. degree in Optical System Technologies from the University of Applied Sciences Ravensburg-Weingarten. After her studies she worked as a research assistant in the collaborative research center ZAFH LED-Oasysat the University of Applied Sciences Ravensburg-Weingarten and achieved her PhD in the faculty of Electrical Engineering of the Karlsruhe Institute of Technology in Germany, which she finished at the end of 2015. Since February 2016 she has been working at Airbus Defence and Space.

Jörg Baumgart
Hochschule Ravensburg Weingarten
Doggenriedstraße, 88250 Weingarten
Germany

Jörg Baumgart received a Dipl.-Ing. (FH) degree in Physics from the Rhein Main University of Applied Sciences in Rüsselheim and a Dipl.-Ing. (TU) degree in Mechanical Engineering from the Technical University of Ilmenau. This was also where he received his Dr-.Ing.. Later on he worked as an optical engineer and optical designer for Diehl BGT Defence in Überlingen. Now he is Professor for Technical Optics at the University of Applied Sciences in Ravensburg Weingarten. He is Vice-Dean of the Faculty for Technology and Management and coordinates the collaborative research center ZAFH LED-Oasys.

Cornelius Neumann
Karlsruhe Institute of Technology
Department of Electrical Engineering and Information Technology, Light Technology Institute, Engesserstr. 13, 76131 Karlsruhe
Germany

Cornelius Neumann studied Physics and Philosophy at the University of Bielefeld, Germany. After his PhD, he worked for the automotive supplier Hella in the advanced development for Automotive Lighting. During his time at Hella he was responsible for signal lighting, LED application and acted as a director of the L-LAB, a laboratory for lighting and mechatronics in public private partnership with the University of Paderborn, Germany. In 2009, he became Professor for Optical Technologies in Automotive and General Lighting and one of the two directors of the Light Technology Institute at the Karlsruhe Institute of Technology, Germany.